

## A 3D Printed Bi-Directional Turbine for Thermoacoustic Standing Wave Environment at an Atmospheric Pressure

Fatimah Al Zahrah Mohd Saat<sup>1,2,\*</sup>, Nurhafizah Nordin<sup>1</sup>, Nur Damia Asma Rosle<sup>1,2</sup>, Safarudin Ghazali Herawan<sup>3</sup>

<sup>1</sup> Fakulti Teknologi dan Kejuruteraan Mekanikal (FTKM), Universiti Teknikal Malaysia Melaka (UTeM), Hang Tuah Jaya, 76100 Durian Tunggal Melaka, Malaysia

<sup>2</sup> Green and Efficient Energy Technology (GrEET), Centre for Advanced Research on Energy (CARE), Universiti Teknikal Malaysia Melaka, Hang Tuah Jaya 76100 Durian Tunggal, Melaka, Malaysia

<sup>3</sup> Industrial Engineering Department, Faculty of Engineering, Bina Nusantara University, Jakarta, 11480, Indonesia

### ABSTRACT

This paper reports a study on the use of an in-house 3D printed bi-directional turbine for energy conversion in a standing wave thermoacoustic environment that is operated at atmospheric pressure. The-3D printed turbine was placed at two locations along the resonator and the data were recorded over a range of flow frequency and flow amplitude. It is found that maximum output is achieved when the flow is not at resonance. Resonance of the standing wave inside the rig was found at 106 Hz but the bi-directional turbine performs better at a lower frequency of 85 Hz.

### Keywords:

Bi-directional turbine; thermoacoustics;  
3D print

Received: 4 Dec. 2023

Revised: 24 Jan. 2023

Accepted: 2 Feb. 2024

Published: 1 Mar. 2024

## 1. Introduction

Renewable energy and technology are becoming more and more important as the world is facing serious issues related to pollution, shortage of fuel supply and ozone depletion [1]. Turbines are devices that can be used to convert kinetic energy of flow into electricity [2]. It is mostly used for harvesting wind [3] and hydrokinetic energy [4]. It is also used in energy production devices like in a geothermal power plant [5] or organic power plant [6]. In more recent development, the turbine with the utilization of appropriate guiding vane have found its use in the field of reciprocating and oscillatory flow condition, a condition that can be found in ocean engineering [7] as well as thermoacoustic technology [8].

A thermoacoustic (TA) systems utilizes thermoacoustic principles to produce either a heating or a cooling effect [9]. Thermoacoustic describes the interplay between heat and sound by combining the principles of thermodynamics, fluid dynamics, and acoustics [10]. Gas particles can expand,

\* Corresponding author.

E-mail address: [fatimah@utem.edu.my](mailto:fatimah@utem.edu.my) (Fatimah Al Zahrah Mohd Saat)

compress, and exchange heat with neighboring surfaces using thermoacoustic principles, completing a thermodynamic cycle and providing a heating/cooling effect [11] as well as heat engine/generator [12]. These interactions may be used to create useful devices that transform heat into sound waves with significant amplitudes when correct conditions are achieved. The work energy in these sound waves can then be utilized to drive a flywheel or a linear alternator with a piston [8]. As a result, a heat engine or a generator is produced using thermoacoustic principles [13]. In an opposite operation, the changes of pressure of the wave and heat transfer between the wave and the surface of porous media can create heat pumping effect where heat is pumped from a lower to a higher temperature reservoir in a thermoacoustic heat pump or refrigerator [14].

The fundamentals of a thermoacoustic engine are the same as those of a thermodynamic engine. When heat is applied to a thermoacoustic engine, the engine produces work in the form of sound while rejecting waste heat into a cooler environment [15]. A thermoacoustic engine comprises no moving parts, making it a viable alternative to traditional engines due to its great reliability and low cost [16]. The whole operations take place entirely within a resonator. As a conclusion, it is an eco-friendlier technology than a standard refrigerator or engine.

In brief, a simple thermoacoustic cooler consisted of a resonator, porous media, acoustic driver and heat exchangers [17]. The acoustic driver drives the acoustic flow inside the resonator and the cooling effect happens when the flow interacted with the porous media [17]. The heat exchanger is used to exchange heat between the system, the cooler and the surrounding [18].

For heat engine or generator, the system is usually driven by a temperature gradient known as the onset temperature that developed between the two ends of the regenerator/porous structure [19]. The onset temperature creates wave that travels inside the resonator and the displacement of the wave can be converted into useful electricity by using suitable energy conversion device [20]. The common device that was used as the energy conversion device was the converted loudspeaker [21] and a linear motor [22]. The bi-directional turbines were used for oscillatory flow of the ocean wave [23]. The potential of using a bi-directional turbine for thermoacoustics was also reported [24]. The bi-directional turbines are self-rectifying turbines that transform the flow's linear oscillating motion to unidirectional rotation, avoiding the zero-velocity point [24]. They are either impulse turbines or response turbines [25]. Printing manufacturing parts with 3d printing technology reduces the production costs [26]. Hence it can be used to fabricate parts for devices [27] such as the bi-directional turbine of thermoacoustics. Moreover, this turbine does not require extensive cooling or the usage of costly magnets [8]. Turbines have proved their utility in conversion wave energy in Oscillating Water Column (OWC) systems, in which they create an oscillating air column because of sea and ocean water movement [23]. The turbine then converts energy to mechanical power.

In bi-direction turbine, the role of the guiding vane, also knowns as stator, and the rotating vane known as rotor is important. The guiding vane guides the fluid to flow into the rotating vane [7]. Three major categories of bidirectional turbines were reported in the literature: the wells turbine [28], the radial impulse turbine [29], and the axial impulse turbine [7]. The axial impulse turbine consists of two guide vanes and a rotor is sandwiched between them. Static guides vanes convert acoustic pressure energy to kinetic energy and send it to the rotor blades. Due to the same size, regardless of the incoming axial flows, the rotor will experience torque in almost the same rotating direction. Then, by coupling the rotor to a generator, the rotor's input power may be converted to electricity. For an impulse radial turbine, the rotor is radially positioned between two guiding vanes, one of which directs the flow outward toward increasing radius and the other inward toward the center axis. The kinetic energy of the bidirectional flow is converted to spinning effort again by a similarly constructed rotor [30].

Recently, bidirectional turbines were developed as potentially low-cost, dependable, and high-performance transducers. In most reported work, the turbines that were investigated were relatively big in size [23–25]. However, most thermoacoustic devices were built by using standard small size pipes [17–19]. In fact, most technology are nowadays becoming small in size and small size operations are usually different compared to the big devices [22]. Hence, there is a need for investigations of small size turbines to suit for the potential use in applications with limitation of space. In this paper, the feasibility of using an in-house 3D printed small size bi-directional turbine to convert acoustical energy from a standing wave thermoacoustic device into electricity is reported and discussed.

## 2. The 3D printed bi-directional turbine

The bi-directional turbine contains three main parts which is the stator at upstream, the rotor at the centre and the stator at downstream. The stator is designed so that the air from upstream and downstream are pushing the rotor into unidirectional motion. The Solidworks drawing of the parts are as shown in Figure 1. The drawings are saved in a stereolithography (STL) format and then send for printing by using Creatbox DX 03 Printer.

For oscillatory motion of thermoacoustic, the air flows in two-directions [31] depending on the cycle of the flow. During first half of the cycle, the air is moving in positive direction. During the second half of the cycle, the air is moving in negative direction [32]. The cycle repeats many times, and the repetition of cycle depends on the frequency of the flow [33]. The stator must be designed with ability to provide continuous flow of air when the oscillatory flow of thermoacoustic is flowing from upstream and downstream locations to rotate the rotor. The rotor is connected to the shaft of a brushless motor to convert the rotational movement into electricity. The motor that was used in the experiment has the ability to handle 200 rpm to 6000 rpm with power voltage of a maximum of 20 V.

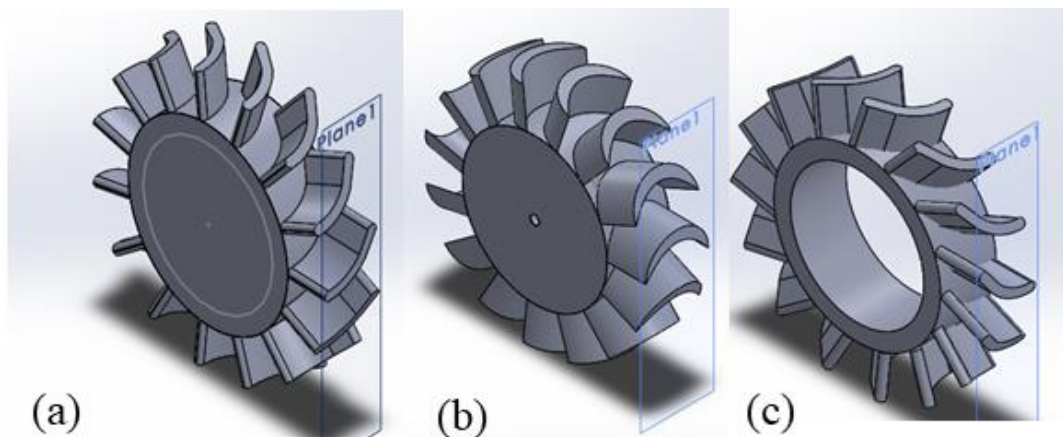


**Fig. 1.** a) The stator on the left (upstream), (b) the rotor in the middle and (c) the stator on the right (downstream)

The dimensions of the stator at both the upstream and downstream locations as well as the rotor are as tabulated in Table 1. All the components are to be fitted into the 30 mm diameter acrylic tube that acts as part of the resonator. For this reason, the stators and rotor of the custom designed bi-directional turbine is made with an outer diameter of approximately 30 mm. The acrylic tube was used as the transparent feature of the tube and this will allow the rotational movement of the rotor to be measured using a device known as a tachometer.

The rotor and stator are placed next to each other as illustrated in Figure 2. There is a 1 mm gap between the rotors and stator to avoid friction between parts when the rotor is rotating. The stator at upstream location does not have inner diameter as the central part is made solid to avoid flow to enter through the middle part of the stator. The stator at downstream location is printed with an inner diameter of 24 mm as it is fitted onto the surface of the 24 mm diameter motor. The inner diameter of the rotor follows the 1.8 mm diameter shaft of the motor.

**Table 1**  
The dimensions for the bi-directional turbine

Parameter	Dimension		
	Stator (upstream)	Rotor	Stator (downstream)
Outer diameter	30 mm	30 mm	30 mm
Inner diameter	-	1.8 mm	24 mm
Number of blades	15	15	15
Length of blades	10 mm	9 mm	10 mm
Angle blade	45°	180°	60°
Thickness of blade	8 mm	13 mm	8 mm
Direction of blade	Static	Clockwise	Static



**Fig. 2.** The assembled 3D printed stator on the left (upstream), the rotor in the middle and the stator on the right (downstream)

The 3D printed bi-directional turbine that is assembled with a motor is then tested in the experimental rig that was built for the study.

### 3. Experimental setup

The experimental rig was based on a quarter wavelength standing wave criteria, similar to the rig as reported in a published work [34]. For a quarter wavelength rig, the rig is made with a length that is equivalent to a quarter of the wavelength. The wavelength can be calculated as  $\lambda = c/f$  where  $c$  is the speed of sound for air which is treated as a constant value of 346 m/s at an atmospheric pressure, and  $f$  is the flow frequency. In general, a thermoacoustic heat engine is a device that generates energy from the acoustic flow that is generated by the heat supply. In this study, the focus is only on the feasibility of using a small sized 3D printed bi-directional turbine to generate electricity when it is rotated by the acoustical flow of thermoacoustics. For this reason, the role of the heat exchangers as the driver for the flow is replaced by another acoustic driver that is a speaker. A 150 W Vess D5 speaker was used to provide the thermoacoustic flow environment in a resonator as illustrated in Figure 3.

The speaker is connected to a 30 mm diameter tube that acts as a resonator. The resonator is made of two different tubes of the same size: the polyvinyl chloride (PVC) tube and the acrylic tube. The bi-directional turbine is placed inside an acrylic tube for measurement purpose. The whole length of the resonator is 725 mm. The speaker is driven by input parameter that is supplied through the use of the MCP SG1005 function generator and the Behringer KM70 power amplifier. This will create a standing wave thermoacoustic environment inside the resonator. The location of the resonator that is attached to the speaker is known as the velocity antinode location whereas the other end of the resonator is known as the pressure antinode location. An Endevco 8510B-2 pressure transducer was flushed mounted on the pressure antinode end so that pressure amplitude data can be recorded. For a standing wave resonator with a quarter wavelength design, the pressure antinode provides maximum amplitude of flow which helps in the determination of resonance frequency for the flow. The pressure transducer is driven by a 12 V power input and the data is transferred to the computer through a D-718-E datalogger. The data is processed by using a Windaq software.

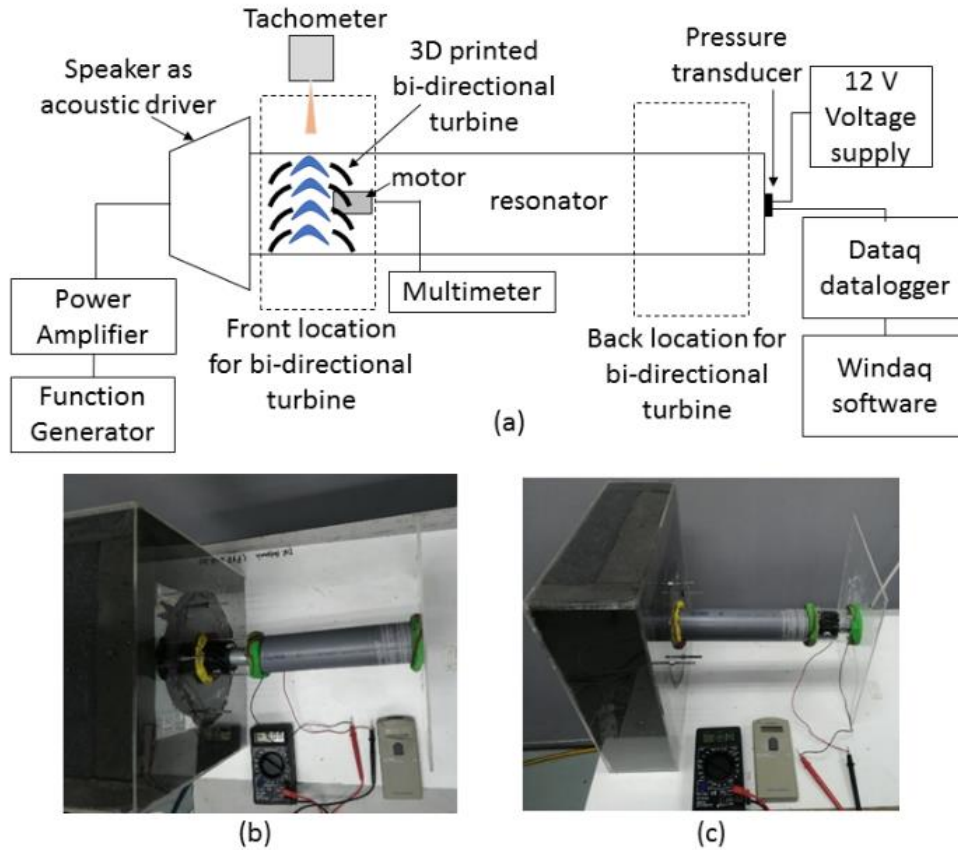


**Fig. 3.** (a) The schematic diagram of the experimental setup, and the picture of the experiment with the bi-directional turbine at (b) the front and (c) at the back of the rig

The bi-directional turbine was located at two different locations: the front location near the velocity antinode and the back location near the pressure antinode. The rotational movement of the bi-directional turbine at these two locations are recorded by using a HT-4200 tachometer. The rotor of the bi-directional turbine is also connected to a DT-830B digital multimeter to record the voltage output from the motor. Each experiment was repeated for at least three times. The uncertainty of experimental data,  $s$ , is calculated by using the following equation [35]:

$$s = \sqrt{\frac{(x_1 - \bar{x})^2 + \dots + (x_n - \bar{x})^2}{n-1}} \quad (1)$$

#### 4. Results and discussions

The results are reported based on all the measurements that are done in the experiment. Discussions are also presented accordingly.

##### 4.1 Resonance Test

Figure 4 presents the results of the resonance frequency of the flow. For thermoacoustics, the flow is usually driven at resonance so that maximum output can be achieved. For a 725 mm long quarter wavelength resonator, theory predicts that the frequency of the flow is about 119 Hz. This theoretical value may change a bit due to experimental losses that may happen. For this reason, the

study started with the identification of the resonance frequency of the flow. This is done by setting the flow amplitude at a constant low value while the frequency varies until the peak value of pressure can be recorded by the pressure that is placed at the pressure antinode location.

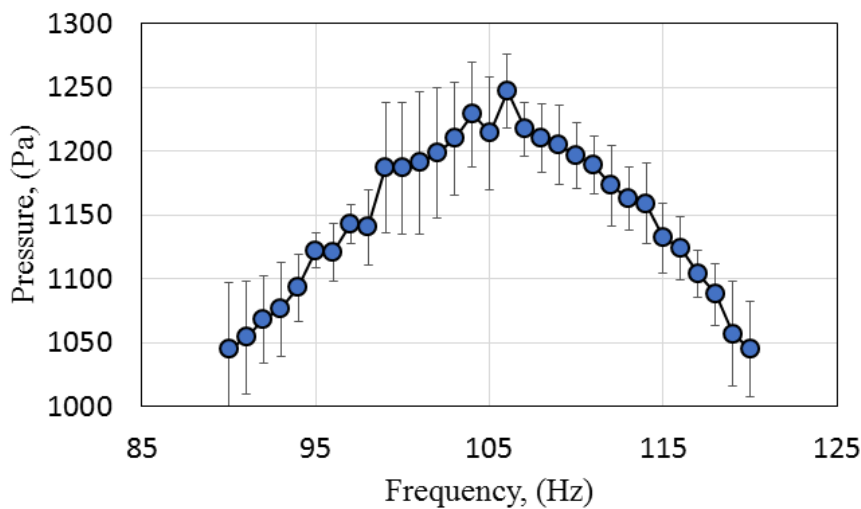


**Fig. 4.** Resonance frequency test for the 725-mm-long quarter wavelength resonator with air at an atmospheric pressure as the working fluid

Figure 4 shows that resonance was achieved at 106 Hz, a value that is 13 Hz lower than the theoretical prediction. Similar observation was also observed in reported works where experimental value was found to be lower than the theoretical prediction [36], presumably due to the uncertainty of the experimental environment such as the nonlinear or inhomogeneous acoustical properties of the materials that were used in the experiment, the errors due to weaknesses in the joints or during assembly practices of parts and also the losses due to the disruption of flow in the presence of porous media, just to name a few.

#### 4.2 Flow amplitude

The investigation is proceeded with the test of flow amplitude in order to ensure that a standing wave acoustic flow is able to be achieved in the resonator. In this test, the pressure data at the location of pressure amplitude is recorded when the input peak-to-peak voltage,  $V_{pp}$ , increases while the flow frequency is set at a constant resonance value of 106 Hz. Figure 5 shows that the pressure amplitude increases when the input voltage increases. This shows that a bigger standing wave amplitude can be achieved by increasing the amplitude of voltage supply. Increasing the amplitude to higher value is not possible due to the limitation of the speaker used in the study. Nevertheless, the range of the pressure values that can be achieved through this experimental setup is sufficient for the test of the custom-designed 3D-printed bi-directional flow turbine. The pressure amplitude at the location of pressure antinode is directly related to the amplitude of flow [28]. The increase of flow amplitude will give impact on the rotational movement of the rotor.

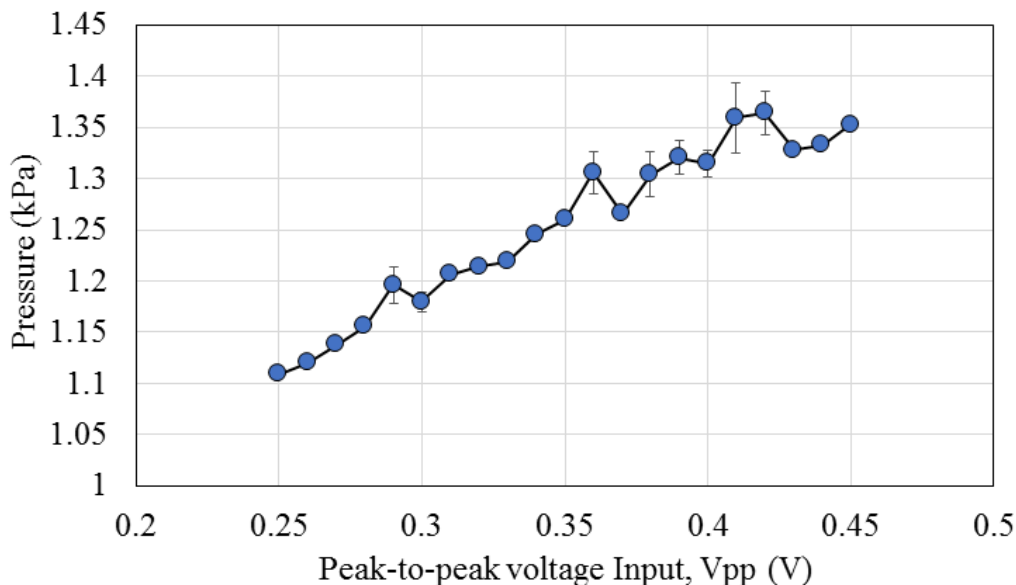


**Fig. 5.** Flow amplitude changes inside the resonator, indicated by the pressure changes, when the peak-to-peak voltage supply is increased from 0.25 V to 0.45 V

In order to confirm the changes of flow amplitude with respect to changes of supply voltage, the resulting velocity of the flow is measured. Our preliminary tests showed that maximum limit of the operation of the motor that was attached to the rotor is reached when the flow is supplied at a peak-to-peak voltage of 0.28 V. Hence, the experimentation involving the use of the custom-made 3D printed bi-directional turbine is carried out to the maximum input peak-to-peak voltage of 0.28 V. For the purpose of illustrating the changes of flow amplitude with the change of pressure amplitude at the antinode, experimentation for a lower  $V_{pp}$  of 0.26 V is also shown. The measurement of flow velocity is done at the front and back locations of the resonator. Data was recorded by using HHF 1000 hot wire anemometer with test conditions set at two different input peak-to-peak flow amplitudes. The flow was first tested with the maximum resonance frequency of 106 Hz. Due to the disturbing noise level of the operations at 106 Hz, the tests were further extended to check for the performance of the flow at frequency lower than the resonance frequency. Two random lower values of frequency were selected which were 55 Hz and 85 Hz. Frequency lower than 55 Hz was not tested due to low production of amplitude that led towards difficulty in obtaining steady operation for meaningful measurement. Extending the experiment for higher frequency was also not considered due to the high noise level which is not favorable for the operation of the system. The results are as tabulated in Table 2. In general, flow amplitude increases when the input supply of peak-to-peak voltage increases except for the case of 106 Hz when measurement is done at the back of the resonator. However, the drop is small and fall within the range of the uncertainty of the velocity experimentation which was calculated to be at approximately  $\pm 0.5$  m/s.

**Table 2**

The velocity of flow at the front and back of the resonator at two different flow amplitudes

Frequency (Hz)	Amplitude of $V_{pp}$ (V)	Velocity Average (m/s)	
		Front location	Back location
55	0.26	1.8600	4.3333
	0.28	2.0800	5.2033
85	0.26	5.0433	3.1367
	0.28	5.6333	3.2467
106	0.26	7.0433	2.9300
	0.28	8.4600	2.3300

It is also interesting to note that the flow behavior at these three different frequencies is different. At low amplitude of 55 Hz, the velocity in front is lower than that at the back. This is different compared to the other two higher flow frequencies. For a standing wave device with quarter wavelength criteria, the velocity of flow is expected to be lower at the back when flow is reaching the pressure antinode. The flow that was observed at the frequency of 55 Hz is not representing this behavior. It is noted that the resonance of flow was recorded at 106 Hz. Therefore, the lower frequency of 55 Hz may be too low to provide thermoacoustic environment by using the current setting.

### 4.3 Voltage Output

Figure 6 shows the output voltage from the bi-directional turbine that is recorded for the conditions reported in Table 1. It is interesting to note that the maximum output voltage was found at a frequency of 85 Hz, and this is not the resonance frequency of the flow.

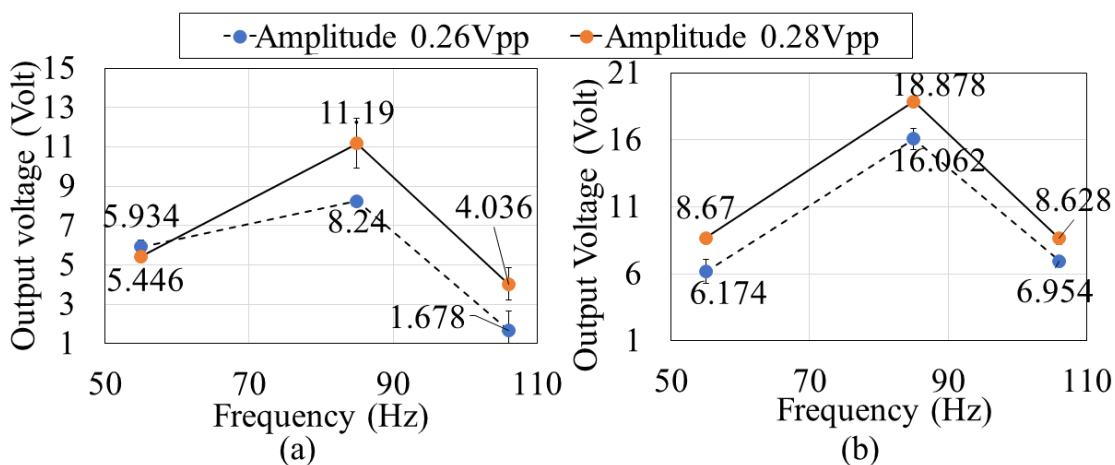


**Fig. 6.** Voltage output from the motor when the turbine is placed (a) in front and (b) at the back of the resonator with different flow frequency operations

The turbine produces more output voltage when it is placed at the back, near the pressure antinode location. The maximum output voltage of 18.88 V was found recorded when the rig is operated at 85 Hz with flow amplitude that is driven with 0.28 peak-to-peak voltage. This indicates that the highest output from the bi-directional turbine can be obtained at a frequency that is not the resonance frequency of the flow.

#### 4.4 Power output

Figure 7 shows the power that is generated by the bi-directional turbine. The results were obtained from data that was recorded for the same conditions as reported in Table 1. The power,  $P$ , in unit Watt is calculated by using the Eq. (2):

$$P = \frac{2\pi N\tau}{60} \quad (2)$$

where the terms  $N$  and  $\tau$  are the speed of the rotor in unit rpm and the torque in unit N.m, respectively. The torque,  $\tau$ , is defined as:

$$\tau = rF \quad (3)$$

Where the terms  $r$ , and  $F$  are the radius of the turbine in unit m, and the centrifugal force in unit Newton. The centrifugal force is calculated using Eq. (4) with  $P$  as the pressure in unit Pa and  $A$  is the cross-sectional area of the rotor in unit  $m^2$ .

$$F = PA \quad (4)$$

The pressure can be obtained by using the measured pressure at the location of pressure antinode,  $P_a$ . The pressure changes with location. The pressure at location  $x$ ,  $P_x$  can be calculated using Eq. (5). The terms  $k$  and  $x$  are the wave number in a unit meter and the location in a unit meter, respectively. The wave number is defined in Eq. (6).

$$P_x = P_a \cos(kx) \quad (5)$$

$$k = \frac{2\pi f}{c} \quad (6)$$

The results of Figure 7 are recorded at two locations. The results for the front location are shown in part (a) of the figure while the results for the back location of the resonator is shown in part (b) of the figure.

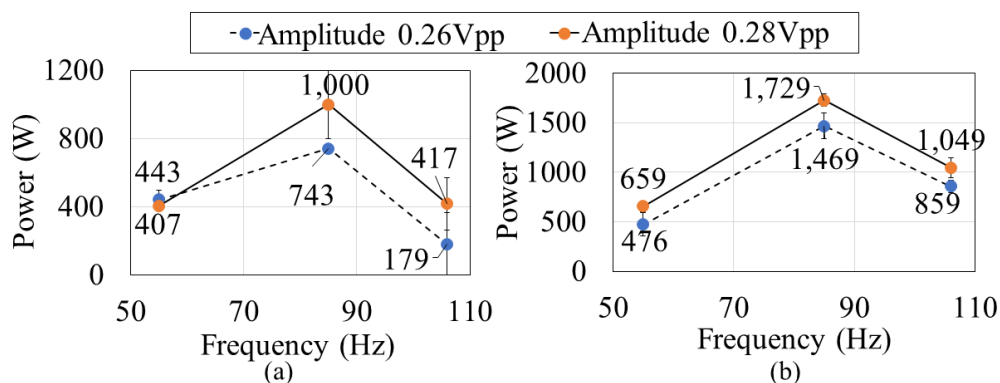


**Fig. 7.** Power generated by the turbine located (a) in front and (b) at the back of the resonator with flow

Again, the results in Figure 7 shows that the maximum output power of the bi-directional turbine is achieved when the system is operated at 85 Hz, which is lower than the resonance frequency of the flow. This is consistent with the results of Figure 6. Higher flow amplitude will also lead to higher power output. The maximum power output of 1.729 kW was recorded when the bi-directional turbine is driven by flow amplitude of 0.28 peak-to-peak voltage with flow at a frequency of 85 Hz.

## 5. Conclusions

A small size 3D printed bi-directional turbine with a diameter of 30 mm was successfully fabricated and tested in a standing wave thermoacoustic environment at an atmospheric pressure operation. Maximum performance was achieved at a frequency of 85 Hz with maximum power of 1.729 kW and a voltage output of 18.88 V. The turbine performed better when it is placed near the pressure antinode location of the standing wave resonator.

## Acknowledgement

The research works are done using facilities at Universiti Teknikal Malaysia Melaka. The work reported here is part of the project funded by the Ministry of Higher Education Malaysia under FRGS/1/2023/TK08/UTEM/02/1.

## References

- [1] Blazy, Rafał, Jakub Błachut, Agnieszka Ciepiela, Rita Łabuz, and Renata Papież. "Renewable energy sources vs. an air quality improvement in urbanized areas-the metropolitan area of Kraków case." *Frontiers in Energy Research* (2021): 657. <https://doi.org/10.3389/fenrg.2021.767418>
- [2] Herlambang, Yusuf Dewantoro, Budhi Prasetyo, Abdul Syukur Alfauzi, Totok Prasetyo, and Fatahul Arifin. "Experimental and simulation investigation on savonius turbine: influence of inlet-outlet ratio using a modified blade shaped to improve performance." (2022): 457-464. <https://doi.org/10.5109/4794172>
- [3] Ismaiel, Amr Mohamed Metwally, Sayed Mohamed Metwalli, Basman Mohamed Nabil Elhadidi, and Shigeo Yoshida. "Fatigue analysis of an optimized HAWT composite blade." (2017): 1-6. <https://doi.org/10.5109/1929656>
- [4] Ren, Hew Wei, Fatimah Al Zahrah Mohd Saat, Fadhilah Shikh Anuar, Mohd Arizam Abdul Wahap, Ernie Mat Tokit, and Tee Boon Tuan. "Computational Fluid Dynamics Study of Wake Recovery for Flow Across Hydrokinetic Turbine at Different Depth of Water." *CFD Letters* 13, no. 2 (2021): 62-76. <https://doi.org/10.37934/cfdl.13.2.6276>
- [5] Prasetyo, Bambang Teguh, M. A. M. Oktaufik, and S. Himawan. "Design, construction and preliminary test operation of bppt-3mw condensing turbine geothermal power plant." (2019): 162-167. <https://doi.org/10.5109/2321012>
- [6] Sharma, Manish, and Rahul Dev. "Review and preliminary analysis of organic rankine cycle based on turbine inlet temperature." (2018): 22-33. <https://doi.org/10.5109/1957497>

- [7] Gato, L. M. C., A. A. D. Carrelhas, and A. F. A. Cunha. "Performance improvement of the axial self-rectifying impulse air-turbine for wave energy conversion by multi-row guide vanes: Design and experimental results." *Energy Conversion and Management* 243 (2021): 114305. <https://doi.org/10.1016/j.enconman.2021.114305>
- [8] Timmer, Michael AG, Kees de Blok, and Theo H. van der Meer. "Review on the conversion of thermoacoustic power into electricity." *The Journal of the Acoustical Society of America* 143, no. 2 (2018): 841-857. <https://doi.org/10.1121/1.5023395>
- [9] Avent, Andrew W., and Chris R. Bowen. "Principles of thermoacoustic energy harvesting." *The European Physical Journal Special Topics* 224, no. 14-15 (2015): 2967-2992. <https://doi.org/10.1140/epjst/e2015-02601-x>
- [10] Jaworski, Artur J., and Xiaoran Mao. "Development of thermoacoustic devices for power generation and refrigeration." *Proceedings of the Institution of Mechanical Engineers, Part A: Journal of Power and Energy* 227, no. 7 (2013): 762-782. <https://doi.org/10.1177/0957650913493622>
- [11] Abd El-Rahman, Ahmed I., Waleed A. Abdelfattah, Karim S. Abdelwahed, Ahmed Salama, Ahmed Rabie, and Ahmed Hamdy. "A compact standing-wave thermoacoustic refrigerator driven by a rotary drive mechanism." *Case Studies in Thermal Engineering* 21 (2020): 100708. <https://doi.org/10.1016/j.csite.2020.100708>
- [12] Mumith, Jurriath-Azmathi, Tassos Karayiannis, and Charalampos Makatsoris. "Design and optimization of a thermoacoustic heat engine using reinforcement learning." *International Journal of Low-Carbon Technologies* 11, no. 3 (2016): 431-439. <https://doi.org/10.1093/ijlct/ctv023>
- [13] Agarwal, Harshal, Vishnu R. Unni, K. T. Akhil, N. T. Ravi, S. Md Iqbal, R. I. Sujith, and Bala Pesala. "Compact standing wave thermoacoustic generator for power conversion applications." *Applied Acoustics* 110 (2016): 110-118. <https://doi.org/10.1016/j.apacoust.2016.03.028>
- [14] Vanapalli, Srinivas, M. E. H. Tijani, and Simon Spoelstra. "Thermoacoustic-Stirling heat pump for domestic applications." In *Fluids Engineering Division Summer Meeting*, vol. 49491, pp. 111-116. 2010. <https://doi.org/10.1115/FEDSM-ICNMM2010-31150>
- [15] Gardner, David L., and Carl Q. Howard. "Waste-heat-driven thermoacoustic engine and refrigerator." In *Proceedings of ACOUSTICS*, pp. 23-25. 2009.
- [16] Backhaus, Scott, and G. W. Swift. "New varieties of thermoacoustic engines." In *Proceedings of the Ninth International Congress on Sound and Vibration*, pp. 8-11. 2002.
- [17] Tijani, M. E. H., J. C. H. Zeegers, and A. T. A. M. De Waele. "Design of thermoacoustic refrigerators." *Cryogenics* 42, no. 1 (2002): 49-57. [https://doi.org/10.1016/S0011-2275\(01\)00179-5](https://doi.org/10.1016/S0011-2275(01)00179-5)
- [18] Sharify, Esmatullah Maiwand, and Shinya Hasegawa. "Traveling-wave thermoacoustic refrigerator driven by a multistage traveling-wave thermoacoustic engine." *Applied Thermal Engineering* 113 (2017): 791-795. <https://doi.org/10.1016/j.applthermaleng.2016.11.021>
- [19] Setiawan, Ikhsan, Wahyu N. Achmadin, Prastowo Murti, and Makoto Nohtomi. "Experimental study on a standing wave thermoacoustic prime mover with air working gas at various pressures." In *Journal of physics: conference series*, vol. 710, no. 1, p. 012031. IOP Publishing, 2016. <https://doi.org/10.1088/1742-6596/710/1/012031>
- [20] Bi, Tianjiao, Zhanghua Wu, Limin Zhang, Guoyao Yu, Ercang Luo, and Wei Dai. "Development of a 5 kW traveling-wave thermoacoustic electric generator." *Applied energy* 185 (2017): 1355-1361. <https://doi.org/10.1016/j.apenergy.2015.12.034>
- [21] Yu, Zhibin, Patcharin Saechan, and Artur J. Jaworski. "A method of characterising performance of audio loudspeakers for linear alternator applications in low-cost thermoacoustic electricity generators." *Applied acoustics* 72, no. 5 (2011): 260-267. <https://doi.org/10.1016/j.apacoust.2010.11.011>
- [22] Liu, Jin, and Steven L. Garrett. "Characterization of a small moving-magnet electrodynamic linear motor for use in a thermoacoustic refrigerator." *The Journal of the Acoustical Society of America* 117, no. 4 (2005): 2386-2386. <https://doi.org/10.1121/1.4785726>
- [23] Otaola, Erlantz, Aitor J. Garrido, Jon Lekube, and Izaskun Garrido. "A comparative analysis of self-rectifying turbines for the mutriku oscillating water column energy plant." *Complexity* 2019 (2019). <https://doi.org/10.1155/2019/6396904>
- [24] Liu, Dongdong, Yanyan Chen, Wei Dai, and Ercang Luo. "Numerical Analysis of Bi-directional Impulse Turbine Performance for Thermoacoustic Power Generators." *Energy Procedia* 158 (2019): 1986-1992. <https://doi.org/10.1016/j.egypro.2019.01.457>
- [25] Timmer, Michael AG, and Theo H. Van Der Meer. "Characterization of bidirectional impulse turbines for thermoacoustic engines." *The Journal of the Acoustical Society of America* 146, no. 5 (2019): 3524-3535. <https://doi.org/10.1121/1.5134450>
- [26] Hossain, Md Aslam, Altynay Zhumabekova, Suvash Chandra Paul, and Jong Ryeol Kim. "A review of 3D printing in construction and its impact on the labor market." *Sustainability* 12, no. 20 (2020): 8492. <https://doi.org/10.3390/su12208492>

- [27] Roslan, Muhammad Nazmi Hadi, Nor Atiqah Zolpakar, Normah Mohd-Ghazali, and Fatimah Al-Zahrah Mohd Saat. "Analysis of 3d printed stack in thermoacoustic cooling." (2021): 131-137. <https://doi.org/10.5109/4372269>
- [28] Kinoue, Y., M. Mamun, T. Setoguchi, and K. Kaneko. "Hysteretic characteristics of Wells turbine for wave power conversion (effects of solidity and setting angle)." *International Journal of Sustainable Energy* 26, no. 1 (2007): 51-60. <https://doi.org/10.1080/14786450701359117>
- [29] Pereiras, B., Castro, F., el Marjani, A., Rodriguez, M.A. "An improved radial impulse turbine for OWC," *Renew. Energy* 36 (5), 1477-1484 (2011). <https://doi.org/10.1016/j.renene.2010.10.013>
- [30] Shehata, Ahmed S., Qing Xiao, Khalid M. Saqr, and Day Alexander. "Wells turbine for wave energy conversion: a review." *International journal of energy research* 41, no. 1 (2017): 6-38. <https://doi.org/10.1002/er.3583>
- [31] Hasbullah, Nurjannah, Fatimah Al Zahrah Mohd Saat, Fadhilah Shikh Anuar, Mohamad Firdaus Sukri, and Patcharin Saechan. "Experimental and numerical studies of one-directional and bi-directional flow conditions across tube banks heat exchanger." *Thermal Science and Engineering Progress* 28 (2022): 101176. <https://doi.org/10.1016/j.tsep.2021.101176>
- [32] Hasbullah, Nurjannah, Fatimah Al Zahrah Mohd Saat, Fadhilah Shikh Anuar, Dahlia Johari, and Mohamad Firdaus Sukri. "Temperature and velocity changes across tube banks in one-directional and bi-directional flow conditions." (2021): 428-437. <https://doi.org/10.5109/4480725>
- [33] Allafi, Waleed Almkhtar, Fatimah Al Zahrah Mohd Saat, and Xiaoan Mao. "Fluid dynamics of oscillatory flow across parallel-plates in standing-wave thermoacoustic system with two different operation frequencies." *Engineering Science and Technology, an International Journal* 24, no. 1 (2021): 41-49. <https://doi.org/10.1016/j.jestch.2020.12.008>
- [34] Rosle, Nur Damia Asma, Fatimah Al Zahrah Mohd Saat, Raja Nor Firdaus Kashfi Raja Othman, Mohamad Firdaus Sukri, and Patcharin Saechan. "The Effect of Porous Materials on Temperature Drop in a Standing Wave Thermoacoustic Cooler." *International Journal of Nanoelectronics & Materials* 15 (2022).
- [35] Lin, Chou Aw, Fatimah Al Zahrah Mohd Saat, and Fadhilah Shikh Anuar. "Heat Transfer for the Oscillatory Flow of Thermoacoustics across an in-Line Tube-Banks Heat-Exchanger." *Heat Transfer Engineering* 44, no. 10 (2023): 865-883. <https://doi.org/10.1080/01457632.2022.2102962>
- [36] Rosle, Nur Damia Asma, Fatimah Al Zahrah MOHD SAAT, Kashfi RAJA OTHMAN, Raja Nor Firdaus, and Irfan ABD RAHIM. "THE IMPACT OF STACK PARAMETERS ON THE TEMPERATURE DIFFERENCE OF A THERMOACOUSTIC COOLER." *Thermal Science* 26 (2022). <https://doi.org/10.2298/TSCI211018073R>